



## Analysis of partially penetrating slug tests in a stratified formation by alternating piezometer and tube methods



Yoshitaka Sakata<sup>a,\*</sup>, Toshikazu Imai<sup>b</sup>, Ryuji Ikeda<sup>c</sup>, Makoto Nishigaki<sup>d</sup>

<sup>a</sup> Environmental System Research Laboratory, Division of Human Environmental Systems, Faculty of Engineering, Hokkaido University, North-13, West-8, Kita-ku, Sapporo, Hokkaido 060-8628, Japan

<sup>b</sup> GM Labo, Inc., 3-6, Nishi-Tenma, Kita-ku, Osaka, Osaka-fu 530-0047, Japan

<sup>c</sup> Division of Earth and Planetary Dynamics, Faculty of Science, Hokkaido University, North-10, West-8, Kita-ku, Sapporo, Hokkaido 060-0810, Japan

<sup>d</sup> Department of Environmental and Civil Design, Faculty of Environmental Science and Technology, Okayama University, Okayama, Japan

### ARTICLE INFO

#### Article history:

Received 7 September 2014

Received in revised form 28 April 2015

Accepted 8 June 2015

Available online 15 June 2015

This manuscript was handled by Corrado Corradini, Editor-in-Chief, with the assistance of Okke Batelaan, Associate Editor

#### Keywords:

Slug tests

Partially penetrating well

Hydraulic conductivity

Sensitivity analysis

Numerical simulation

Heterogeneity

### SUMMARY

In partially penetrating slug tests, hydraulic conductivity ( $K$ ) estimates might not necessarily be valid because of vertical flows in heterogeneous formations. We assess the error in hypothetical stratified formations by numerical sensitivity analysis, and propose an effective method for compensation by incorporating two types of casing configuration (piezometer and tube). The hypothetical stratified formation consists of completely horizontal layers, each 1 m thick; the permeability is different between, but not within, layers. In this study, conductivity estimates in the piezometer and tube methods are calculated by assigning various patterns of conductivity to the test, upper, and lower layers:  $K_T$ ,  $K_U$ , and  $K_L$ . The effect of vertical flow becomes significant when  $K_T$  is small relative to  $K_U$  or  $K_L$ , and  $K_L$  is more important than  $K_U$  because the base of the borehole is open to the lower formation. The conductivity ratios (estimate over actual value) are treated as approximately linearly dependent on logarithms of  $K_T/K_U$  and  $K_T/K_L$ , so that conductivity estimates can be straightforwardly derived from one piezometer measurement and two tube measurements at the top and bottom of the screen. The linear relations are evaluated and constant parameters are determined under specific conditions. This study also recommends alternating piezometer and tube methods in the drilling procedure because the actual variation of  $K$  with depth is larger than that found using isolated measurements, as shown in a field study of alluvial fan gravel deposits in Sapporo, Japan.

© 2015 Elsevier B.V. All rights reserved.

### 1. Introduction

Slug tests are employed in both practical engineering and scientific studies to determine in situ hydraulic conductivity,  $K$ , by measuring the recovery of head in a single borehole after artificially raising or lowering the water level in the well. Although slug tests are sensitive to artificial and natural conditions in the well (e.g., Black, 2010), they are useful because they are simpler, cost less, and require less equipment than multiple pumping tests. It is also common for slug tests to have a logistical advantage, especially in groundwater contamination investigations. One reason is that slug tests can be conducted without removing or adding water, by lowering a solid piece of metal, called a slug, into a well, which does not disturb the site of suspected contamination. Another reason is that slug test results are related mainly to permeability on a small scale, and thus local information is directly relevant to

preferential flow paths for contamination plumes. In addition, a series of slug tests at multiple depths aids in interpreting vertical variations of  $K$ . When such vertical profiles are interpolated among different locations, three dimensional distributions of  $K$  can be obtained for an individual site. Various previous studies have shown the spatial variability in  $K$  obtained from slug test analyses (Zlotnik and Zurbuchen, 2003; Zemansky and McElwee, 2005; Ross and McElwee, 2007; Leek et al., 2009; Cardiff et al., 2011).

Analytical solutions for slug tests have been available since the work of Hvorslev (1951), and theoretical and numerical studies have contributed to the practical application of slug tests in a variety of conditions for target aquifers (e.g., confined or unconfined), well types (e.g., fully or partially penetrating wells), falling head data (e.g., normally overdamped or nonlinear oscillatory head data), and borehole configurations (e.g., skin or no skin effects), as summarized by Butler (1997). Even in the last decade, analytical solutions of slug tests have been developed, for example, for highly permeable formations (Butler and Zhan, 2004), varying pressure conditions (Chen and Wu, 2006), and unconfined aquifers with

\* Corresponding author. Tel./fax: +81 11 706 6288.

E-mail address: [y-sakata@eng.hokudai.ac.jp](mailto:y-sakata@eng.hokudai.ac.jp) (Y. Sakata).

## Nomenclature

$a_1, b_1, c_1, a_2, c_{2U}, b_2,$ and $c_{2L}$	empirical parameters determined by numerical simulation	$\tilde{K}_{SU}$	hydraulic conductivity estimate obtained by the upper tube method ( $L T^{-1}$ )
$d_c$	diameter of well casing (L)	$\tilde{K}_T$	hydraulic conductivity estimate obtained by alternating the piezometer and tube methods ( $L T^{-1}$ )
$d_s$	diameter of well screen in the piezometer method (L)	$n$	total number of horizontal layers consisting of the formation
$H$	drawdown of hydraulic head in the well during slug tests (L)	$r$	radial coordinate with origin at base of well (L)
$H_0$	initial drawdown of hydraulic head at slug tests (L)	$P$	capillary pressure (L)
$H_1$	drawdown of hydraulic head at the beginning time for analysis (L);	$Q_g$	groundwater discharge rate during slug tests into the well ( $L^3 T^{-1}$ )
$H_2$	drawdown of hydraulic head at the end time for analysis (L)	$R_U$	logarithm of ratio of upper adjoining conductivity to target conductivity; $K_U/K_T$
$L$	length of screen interval in the piezometer method (L)	$R_L$	logarithm of ratio of lower adjoining conductivity to target conductivity; $K_L/K_T$
$K$	hydraulic conductivity ( $L T^{-1}$ )	$\tilde{R}_L$	estimated logarithm of ratio of lower conductivity to target conductivity
$K_i$	hydraulic conductivity in the $i$ th layer from the top to the bottom of the numerical model ( $L T^{-1}$ )	$S_s$	specific storage coefficient ( $L^{-1}$ )
$K_L$	hydraulic conductivity in the lower adjoining layer ( $L T^{-1}$ )	$S_w$	degree of saturation (%)
$K_{Li}$	hydraulic conductivity in the $i$ th layer upper from the test layer ( $L T^{-1}$ )	$t$	time (T)
$K_r$	radial component of hydraulic conductivity ( $L T^{-1}$ )	$T$	time interval for slug test analysis (T)
$K_T$	hydraulic conductivity in the layer to be tested by the piezometer method ( $L T^{-1}$ )	$T_0$	basic time lag at which a normalized head of 0.37 (T)
$K_U$	hydraulic conductivity in the upper adjoining layer ( $L T^{-1}$ )	$z$	vertical coordinate (L)
$K_{Ui}$	hydraulic conductivity in the $i$ th layer upper from the test layer ( $L T^{-1}$ )	$\alpha$	dimensionless storage parameter, $(2d_s^2 S_s L)/d_c^2$
$K_z$	vertical component of hydraulic conductivity ( $L T^{-1}$ )	$\alpha_L$	ratio of estimate by the piezometer method to by the upper tube method, $\frac{\tilde{K}_{HV}}{K_{SU}}$
$\tilde{K}_{HV}$	estimate of hydraulic conductivity in the piezometer method ( $L T^{-1}$ )	$\alpha_U$	ratio of estimate by the piezometer method to by the lower tube method, $\frac{\tilde{K}_{HV}}{K_{SL}}$
$\tilde{K}_{HV}$	hydraulic conductivity estimate obtained by the piezometer method ( $L T^{-1}$ )	$\theta$	volumetric water content
$\tilde{K}_{SL}$	hydraulic conductivity estimate obtained by the lower tube method ( $L T^{-1}$ )	$\psi$	square root of the anisotropy ratio over the aspect ratio, $\frac{\sqrt{K_z/K_r}}{2L/d_s}$

wellbore inertial effects and well skins (Malama et al., 2011). However, most previous studies of slug tests have been based on the assumption of homogeneity: that is, any flow parameters are constant. This idealized view of formations is not necessarily realistic in nature, and hydraulic properties are often variable to a considerable degree in geologic settings. For example,  $K$  in coarse mixtures ranges over several orders of magnitude, depending on grain sizes and the volume fractions of each component (Koltermann and Gorelick, 1995). However, to our knowledge, only a few studies have discussed the application of slug tests in naturally heterogeneous formations. Karasaki et al. (1988) presented rigorously analytic solutions of fully penetrating slug tests in a formation that contains two layers of different permeability with no vertical flows. In this case, slug test results entirely agreed with those from a homogeneous formation, for which  $K$  was the thickness-weighted arithmetic average, when the vertical flows were neglected. Due to the complexity of aquifer and boundary conditions, numerical approaches offer more flexibility than theoretical studies for handling vertical flow. For example, Beckie and Harvey (2002) numerically examined fully penetrating slug tests with stochastic realizations of  $K$ , and used the solution reported by Cooper et al. (1967) for simulated head recovery data in each realization. As a result, these solutions approximately corresponded to the geometric means of  $K$  in the support volume of slug tests, but were close to the arithmetic means when the characteristic scale of heterogeneity (correlation scale of  $K$ ) increased. On the other hand, partially penetrating slug tests are more affected by vertical flows from the lower adjoining layers than fully

penetrating slug tests. As an example of a typical field study, Shapiro and Hsieh (1998) performed double-packer slug tests in the crystalline fractured rock of central New Hampshire. They found that the water responses in the analytical models are different from the measured responses, probably due to non-radial flow in the vicinity of the borehole. Yu and Lloyd (1992) used several optimization procedures to compensate for the effects of vertical flows in double-packer slug test results under the assumption of multiple layered systems. The effect of vertical flow in partially penetrating slug tests was discussed through a comparison between semi-analytical and conventional solutions (Hyder et al., 1994). Hyder et al. found that the effect was large for small aspect ratios  $2L/d_s$ , where  $L$  is the screen interval length and  $d_s$  is the borehole diameter, as shown later in Fig. 2. Furthermore, Butler et al. (1994) used numerical simulation to evaluate the effect in a horizontally layered formation. They considered the case of multi-level double-packer slug tests and assumed that the hypothetical formation contained horizontal layers of various thicknesses, but with two types of  $K$ . They found that slug test results corresponded approximately to a thickness-weighted average of  $K$  in cases where the test interval spans a number of layers. The conclusion matches that of the study of fully penetrating slug tests described above. The study also revealed that considerable error may be introduced into the estimate of  $K$ , owing to the effects of adjoining layers, when the test interval length was of the order of the average layer thickness. However, this study examined only one set of permeabilities, and the effects of adjoining layers were not examined for various patterns of  $K$  variation. In addition, the

measurement error is assessed only in the double-packer system, but an assessment is also needed in other configurations, such as when both screen and base are open, which is the case for the installation of a casing pipe in a borehole, as is usual in shallow groundwater investigations.

The purpose of this study is to assess the effects of vertical flows on partially penetrating slug tests in horizontally stratified formations, and to propose an efficient method for inferring reasonable estimates of  $K$  in a borehole. The concept in this proposed method is to incorporate different test results in terms of vertical positions of an impermeable casing pipe. Fig. 1 shows definition sketches of test configurations in the hypothetical stratified layers. The ideal formation consists of horizontally infinite layers. As in Butler et al. (1994), hydraulic conductivity  $K$  was variable between layers, but not within each layer, and the vertical ( $K_z$ ) and radial ( $K_r$ ) components of hydraulic conductivity may differ. This study considers test configurations of casing installations; in one the test screen interval is open to the formation, which is called the “piezometer” method, and in the other it is closed (only the bottom is open), which is called the “tube” method. It is noted that the term “piezometer” is used for a well with a finite length of screen, as shown in Fig. 5.21 of Fetter (2001); although one may also use this term for a well of zero screen length (e.g., Freeze and Cherry, 1979), the term “tube” is used instead in this study. Fig. 1 also indicates schematic flow patterns in both methods. The groundwater flows are dominant around the open screen in the radial direction when using the piezometer method, but in the spherical direction when using the tube method; the measurement error due to vertical flow components in the stratified formation is different between the methods. For both methods, a vertical series of slug test results can be obtained without incurring special costs, by incrementally installing casing pipes during drilling. This study also divides the tube method into two types; the bottom is set to the uppermost depth of the screen interval for the piezometer method, the “upper tube method (Fig. 1a)”; and to the lowermost depth, the “lower tube method (Fig. 1c).” The definition is because slug test results might be influenced in the hypothetical formation by hydraulic

conductivity values in the test layer, and upper and lower adjoining layers; compensation will be required in at least three different measurements, because actual conductivity values are not known a priori in most cases. This study aims to construct a simple method for field practitioners to compensate for the conventional measurements by incorporating the piezometer, upper tube and lower tube methods.

The contents of the study are as follows: (1) state the problem and approach of the study, (2) introduce conventional solutions of the piezometer and tube methods for error assessment; (3) derive the two assumptions and propose an effective method by alternating the piezometer and tube methods; (4) perform numerical sensitivity analysis to evaluate the assumptions and to determine constant parameters, for anisotropic and isotropic conditions; (5) show that this method efficiently contributes to estimating vertical variations of  $K$ , by using a field example of alluvial fan gravel deposits in Sapporo, Japan.

## 2. Methodology

### 2.1. Problem statement

This study assesses the measurement error in conventional solutions of piezometer and tube methods, due to vertical flows of groundwater in the horizontally stratified formation, as illustrated in Fig. 1. The hypothetical stratified formation is a reasonable representation for considering the influences of geologic heterogeneity on partially penetrating slug tests. This is because the effective radius of slug tests is relatively small, with a material volume on a scale between 0.1 and 100 m<sup>3</sup> (Rovey and Cherkauer, 1995). The correlation scale of  $K$  in geologic material was smaller than this effective radius in the horizontal direction (tens of meters) and was the same or smaller in the vertical direction, as shown in Fig. 6.6 of Gelhar (1993). This study also assumes that the thickness of each layer is constant and the same with the screen length  $L$  for piezometer method, although the vertical scale of hydraulic conductivity is variable according to sedimentary textures. This assumption is based on the previous study results; slug test results are sensitive to heterogeneity at the same scale with the screen length, and insensitive to that at the smaller scale within the screen length (Butler et al., 1994).

The problem of interest is that of the head response to the instantaneous introduction of a slug of water at a central well in the hypothetical stratified formation, where hydraulic conductivity  $K$  varies between layers, but not within them. Here, we use cylindrical coordinates:  $r$  is the radial coordinate from the center vertical axis of a well,  $z$  is the vertical coordinate from the base of the formation, and  $t$  is the time from the beginning of slug tests. For more generality, when hydraulic conductivity  $K$  is a function of  $z$ , the partial differential equation representing the flow of groundwater in the piezometer method is represented as

$$K_r \frac{\partial^2 h}{\partial r^2} + \frac{K_r}{r} \frac{\partial h}{\partial r} + \frac{\partial}{\partial z} \left( K_z \frac{\partial h}{\partial z} \right) = S_s \frac{\partial h}{\partial t} \quad (1)$$

where  $h$  is the drawdown of water head from the initial head ( $L$ ),  $K_r$  and  $K_z$  are the hydraulic conductivity ( $L T^{-1}$ ) in the radial and vertical components, respectively, and  $S_s$  is the specific storage coefficient ( $L^{-1}$ ).

Initial conditions are

$$h(r, z, 0) = 0, \quad d_s/2 < r < \infty, \quad 0 \leq z \leq nL \quad (2)$$

$$h(d_s/2, z, 0) = H_0, \quad iL \leq z \leq (i+1)L \text{ or } 0, \text{ elsewhere} \quad (3)$$

$$h(r, iL, 0) = H_0, \quad 0 \leq r \leq d_s/2 \quad (4)$$

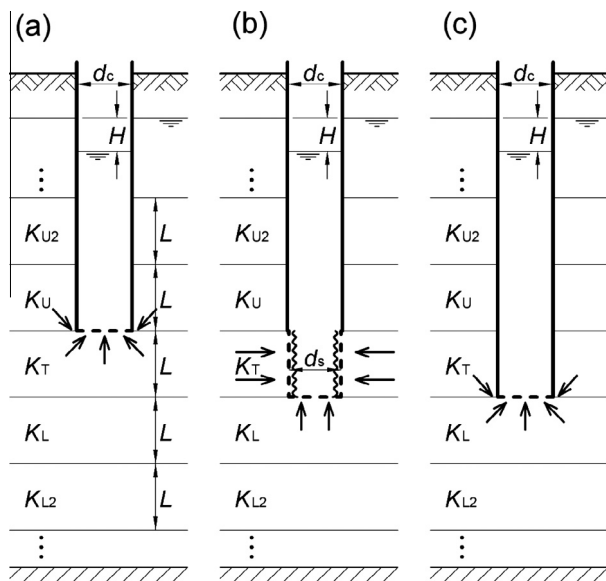


Fig. 1. Cross section of the hypothetical stratified formation and schematic illustration of slug tests using the piezometer (b) and upper (a) and lower (b) tube methods.  $K_r$  denotes radial hydraulic conductivity in the layer to be tested with the piezometer method.  $K_U$  and  $K_L$  denote radial hydraulic conductivities in the upper and lower layers adjoining the test layer, respectively. Subscript  $i$  ( $i = 2, 3, \dots$ ) indicates the number of layers above or below the test layer. Parameters  $d_s$  and  $d_c$  denote the diameters of the test screen and casing pipe, respectively ( $d_s = d_c$  in the tube method).

where  $nL$  is the thickness of the aquifer ( $L$ ),  $n$  is the total number of horizontal layers,  $i$  is the layer number for the test interval ( $L$ ), and  $d_s$  is the diameter of the well screen in a borehole.

The boundary conditions are

$$h(\infty, z, t) = 0, \quad t > 0, \quad 0 \leq z \leq nL \quad (5)$$

$$\frac{\partial h(r, 0, t)}{\partial z} = \frac{\partial h(r, nL, t)}{\partial z} = 0, \quad d_s/2 < r < \infty, \quad t > 0 \quad (6)$$

$$h(d_s/2, z, t) = H, \quad t > 0, \quad iL \leq z \leq (i+1)L \quad (7)$$

$$\begin{aligned} \pi d_s K_r \int_{iL}^{(i+1)L} \frac{\partial h(d_s/2, z, t)}{\partial r} dz + 2\pi K_z \int_0^{d_s/2} r \frac{\partial h(r, iL, t)}{\partial r} dr \\ = \pi (d_c/2)^2 \frac{dH}{dt} = Q_g(t), \quad t > 0 \end{aligned} \quad (8)$$

$$\frac{\partial h(0, z, t)}{\partial r} = 0, \quad t > 0, \quad 0 \leq z \leq iL, \quad (9)$$

$$\frac{\partial h(d_c/2, z, t)}{\partial r} = 0, \quad t > 0, \quad (i+1)L \leq z \leq nL \quad (10)$$

where  $Q_g$  is the groundwater discharge into the well ( $L^3 T^{-1}$ ),  $H$  is the drawdown at time  $t$  in the well, and  $d_c$  is the diameter of the casing pipe ( $L$ ). The initial and boundary conditions are different in Eqs. (4) and (8) from those in Butler et al. (1994), which considered the double-packer slug tests.

The solutions in Eqs. (1)–(10) could be obtained using analytical techniques, which might require several assumptions for simplification; however, to our knowledge, no rigorously analytic solutions have been derived yet, as indicated by Butler (1997). In contrast, for well-pumping problems with constant discharge, several studies have derived solutions for leaky multi-layered systems (Maas, 1987; Cheng and Morohunfolu, 1993; Hemker, 1999). The solutions were formulated in the conventional way for the generality in terms of vertical heterogeneity, but were not straightforward except in limited simple conditions due to their complexity and computational cost.

The proposal in this study was based on a simple relation in terms of measurement errors and intended for practical use to compensate in a vertical series of slug test results more efficiently than by theoretical approaches. The relation was originally indicated in the previous study of Hyder et al. (1994). Hyder et al. derived a semi-analytical solution that considered vertical flow components more rigorously than other conventional solutions, such as that in Hvorslev (1951). This study also compared conductivity estimates from both methods, as shown in Fig. 2, which shows that the Hvorslev estimates  $\tilde{K}_{HV}$  are different from the analytic solutions that depend on two parameters,  $\psi$  and  $\alpha$ , and that the conductivity ratio  $\tilde{K}_{HV}/K$  is approximately linear to the logarithm of  $\psi$  for all  $\alpha$ . It is suggested that the linear relation was due to an increase in vertical flows as  $\psi$  increases, because  $\psi$  reflects the proportion of vertical flow to radial flow in the slug-induced flow system. This study expanded the linear relation in the homogeneous formation to that in the hypothetical horizontally formation; the vertical to horizontal proportion of flow was considered to be that of hydraulic conductivity, namely,  $K_U/K_T$  and  $K_L/K_T$ . Thus, the ratio  $\tilde{K}_{HV}/K$  could be represented as a linear relation with logarithms of  $K_U/K_T$  and  $K_L/K_T$ , which allows error compensation to be performed readily with direct measurements and simple calculations, as described below.

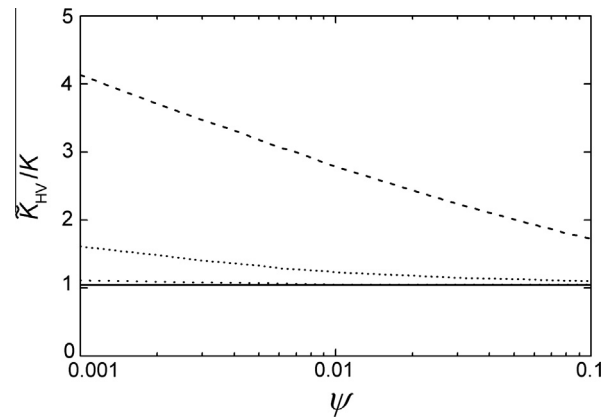


Fig. 2. Plot of conductivity ratio (Hvorslev estimate,  $\tilde{K}_{HV}$ , over actual conductivity,  $K$ ) versus  $\psi$  ( $(K_z/K_r)^{1/2}/(2L/d_s)$ ), modified from Fig. 3 of Hyder et al. (1994). Four lines are obtained from the top at  $\alpha = 0.1, 10^{-3}, 10^{-5}, 10^{-7}$ , respectively.  $\alpha$  is the dimensionless storage parameter ( $(2d_s^2 S_s L)/d_c^2$ ). It is noted that the results were obtained assuming vertical homogeneity and isotropy ( $K_z = K_r$ ).

### 2.2. Conventional solutions of piezometer and tube methods

In this study, the most common Hvorslev (1951) method was used for the assessment, as in Hyder et al. (1994). As compared with other methods (e.g., Cooper et al., 1967), the method is less accurate due to an assumption that aquifer storage is negligible. However the method has an advantage in terms of data analysis, especially for this study, over other types of curve matching. The Hvorslev method for the analysis of partially penetrating slug tests is applied with the shape factor of case 8, which is a well with a screened interval of finite length located in a uniform, vertically unbounded, aquifer with a horizontal to vertical anisotropy in  $K$ . The hydraulic conductivity is given by

$$\tilde{K}_{HV} = \frac{d_c^2}{8LT_0} \log \left( \frac{1}{\psi} + \sqrt{1 + \left( \frac{1}{2\psi} \right)^2} \right) \quad (11)$$

This study considered isotropic and anisotropic conditions in each layer; in the isotropic conditions, the anisotropy ratio  $K_z/K_r = 1$ , whereas in the anisotropic conditions,  $K_z/K_r = 0.1$  (in this study).  $T_0$  is the basic time lag at which a normalized head (measured as drawdown of head  $H$  in a well divided by the initial drawdown  $H_0$ ) of 0.37 is reached. The time lag can be obtained by fitting a straight line to plots of  $\log H$  versus  $t$ , and thus the inverse time lag can be replaced by the slope,  $\log(H_1/H_2)/T$ , where  $H_1$ , and  $H_2$  ( $0 < H_2 < H_1 < H_0$ ) are the drawdowns of head at the beginning and end of time interval  $T$ .

The tube method is less frequently used than the piezometer method, and fewer studies have discussed analytic solutions of the tube method. Kono and Nishigaki (1983) examined five solutions for the tube methods in numerical simulations, and concluded that the Schmidt equations (1967) provided the most reasonable estimates in terms of agreement with actual values. In the Schmidt solution, hydraulic conductivity,  $\tilde{K}_{SU}$  or  $\tilde{K}_{SL}$ , was estimated based on the assumption of spherical flows around the open base of the borehole as

$$\tilde{K}_{SU} = \tilde{K}_{SL} = \frac{d_c \log(H_1/H_2)}{8T} \quad (12)$$

where  $T$  denotes the time interval during which the water level in the borehole rises from height  $H_1$  to  $H_2$ . Note that Eq. (12) does not depend on isotropy or anisotropy. In this numerical simulation, the slope,  $\log(H_1/H_2)/T$ , in Eqs. (11) and (12) was calculated by using simulated slug test data and an automated regression routine. However, Eqs. (11) and (12) could provide inaccurate estimates of  $K$

due to geologic heterogeneity, which this study conceptualized as the horizontally stratified formation.

2.3. Compensation method incorporating piezometer and tube methods

Two basic assumptions are used in this study. (1) Estimated conductivity in the piezometer method,  $\tilde{K}_{HV}$ , is affected by  $K_T$  in the test layer,  $K_U$  in the upper adjoining layer, and  $K_L$  in the lower adjoining layers. In contrast, estimated conductivity in the upper (or lower) tube methods,  $\tilde{K}_{SU}$  (or  $\tilde{K}_{SL}$ ) is affected by  $K_T$  in the test layer and  $K_U$  ( $K_L$ ) in the upper (lower) adjoining layers. The effect of further upper and lower layers,  $K_{U_i}$  and  $K_{L_i}$  ( $i \geq 2$ ), is negligible. (2) Error in the estimates arising from the vertical flows is represented as a ratio of estimates over actual conductivity in the test layer,  $\tilde{K}_{HV}/K_T$ ,  $\tilde{K}_{SU}/K_T$ , and  $\tilde{K}_{SL}/K_T$ . The ratios are approximately linear to the logarithms of  $K_U/K_T$  and  $K_L/K_T$ , through determining the optimal parameters in numerical sensitivity analysis. Under these assumptions, the estimated  $\tilde{K}_{HV}$ ,  $\tilde{K}_{SU}$ , and  $\tilde{K}_{SL}$  values could be represented individually by a set of linear equations,

$$\frac{\tilde{K}_{HV}}{K_T} = a_1 \log\left(\frac{K_U}{K_T}\right) + b_1 \log\left(\frac{K_L}{K_T}\right) + c_1 = a_1 R_U + b_1 R_L + c_1 \quad (13)$$

$$\frac{\tilde{K}_{SU}}{K_T} = a_2 \log\left(\frac{K_U}{K_T}\right) + c_2 = a_2 R_U + c_{2U} \quad (14)$$

$$\frac{\tilde{K}_{SL}}{K_T} = b_2 \log\left(\frac{K_L}{K_T}\right) + c_{2L} = b_2 R_L + c_{2L} \quad (15)$$

where  $R_U$  and  $R_L$  are the logarithms of  $K_U/K_T$  and  $K_L/K_T$ , respectively, and  $a_1, b_1, c_1, a_2, c_{2U}, b_2,$  and  $c_{2L}$  denote constant parameters, which are optimally determined by numerical simulation for various  $K$  patterns. Eq. (13) can be divided by Eqs. (14) and (15) to give

$$\alpha_U = \frac{\tilde{K}_{HV}}{\tilde{K}_{SU}} = \frac{a_1 R_U + b_1 R_L + c_1}{a_2 R_U + c_{2U}} \quad (16)$$

$$\alpha_L = \frac{\tilde{K}_{HV}}{\tilde{K}_{SL}} = \frac{a_1 R_U + b_1 R_L + c_1}{b_2 R_L + c_{2L}} \quad (17)$$

Thus,  $R_U$  and  $R_L$  can be determined from the measurement ratios,  $\alpha_L$  and  $\alpha_U$ , as

$$R_U = \frac{(b_1 - \alpha_L b_2)(c_1 - \alpha_U c_{2U}) - (c_1 - \alpha_L c_{2L})b_1}{a_1 b_1 - (a_1 - \alpha_U a_2)(b_1 - \alpha_L b_2)} \quad (18)$$

$$R_L = \frac{(a_1 - \alpha_U a_2)(c_1 - \alpha_L c_{2L}) - (c_1 - \alpha_U c_{2U})a_1}{a_1 b_1 - (a_1 - \alpha_U a_2)(b_1 - \alpha_L b_2)} \quad (19)$$

Consequently, if the linear relations in Eqs. (13)–(15) were known with sufficient accuracy in the parameter estimation, actual conductivity in the target layer could be estimated straightforwardly by incorporating three different estimates:  $\tilde{K}_{HV}$ ,  $\tilde{K}_{SU}$ , and  $\tilde{K}_{SL}$ . This study also recommends a series of slug tests in a borehole, alternating the piezometer and tube methods over a constant interval in depth and iterating this straightforward method, so that the vertical distribution of  $K$  could be estimated more accurately than from isolated measurements.

2.4. Sensitivity analysis and parameter estimation

In this study, a numerical simulation approach was employed to validate two assumptions and to determine the constant parameters in Eqs. (13)–(15). Fig. 3 shows the cross-sectional and axisymmetric finite-element model used for this analysis. The numerical model consisted of 11 horizontal layers, each 1 m thick ( $L = 1$ ).  $K_i$  ( $i = 1, 2, \dots, 11$ ) are radial hydraulic conductivities, and the subscript number  $i$  begins at the top layer. Each horizontal layer is vertically divided into 10 segments of rectangular finite

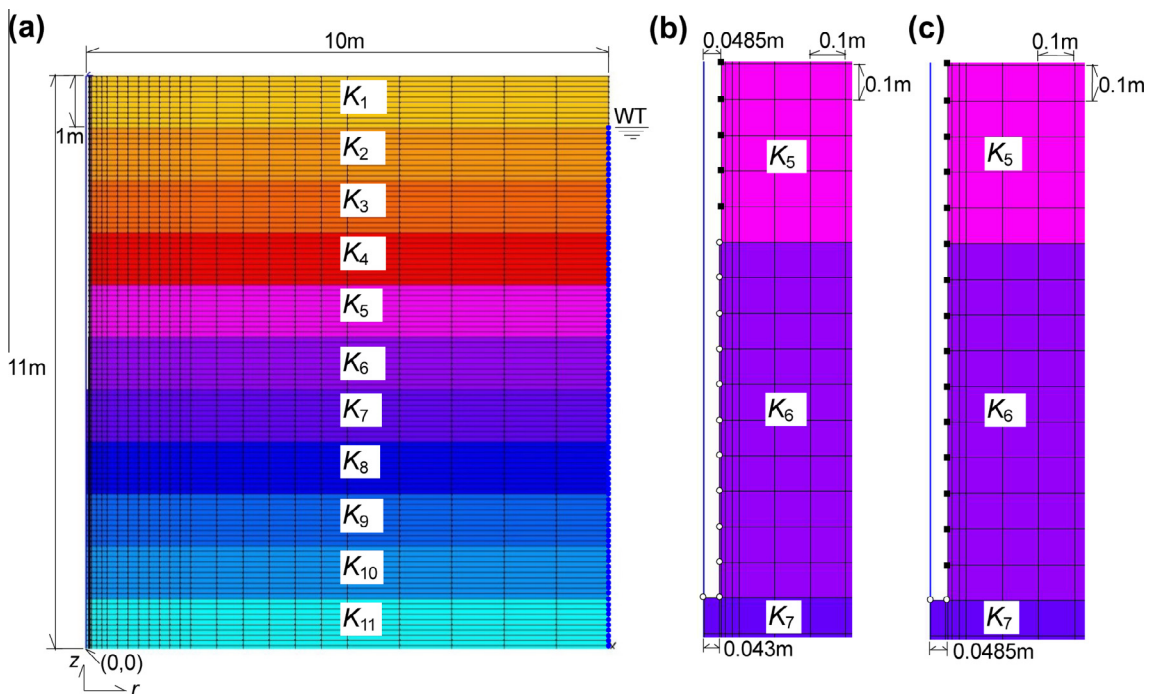


Fig. 3. The radial-flow two-dimensional finite difference model for this analysis. The whole model (a), and expansions of the left side around the horizontal axis of the coordinate system for the piezometer method (b), and the lower tube method (c). WT denotes water table as an initial water level. Solid blue circles along the right side are assigned as constant head boundary conditions. Open blue circles along the well screen are assigned as variable head boundary conditions. Black circles along the casing pipe are assigned as no-discharge (impermeable) conditions. (For interpretation of the references to color in this figure legend, the reader is referred to the web version of this article.)

elements. The horizontal extent is 10 m. The extent should be large enough to contain the effective radius, which depends on the spatial variability of both permeability and storage parameters (Beckie and Harvey, 2002). Therefore, this study examined the effect, and simulated head data commonly showed that the distance of a drawdown over 0.01 m from an initial head was less than several meters, so the horizontal extent of 10 m was large enough relative to the effective radius of slug tests (some examples are omitted due to length restrictions). The left boundary of the model was assumed to be the central axis of the borehole, and the diameters of the screen,  $d_s$ , and casing pipe,  $d_c$ , were assumed to be 86 and 90 mm, respectively. These dimensions are widely used in geotechnical investigations in Japan. The horizontal mesh size is the finest (5.5 mm) along the left side, and grows geometrically away from the axis, finally reaching 1 m. The numerical model is horizontally divided into 20 segments, and the total number of segments is 2970 in this model.

The test screen interval for the piezometer method was assigned to the center of the formation, that is, the 6th layer between 5 and 6 m in depth;  $K_{U2}$ ,  $K_U$ ,  $K_T$ ,  $K_L$ , and  $K_{L2}$  in Fig. 1 correspond to  $K_4$ ,  $K_5$ ,  $K_6$ ,  $K_7$ , and  $K_8$  in this model, respectively. The recovery of water level  $h(r, z, t)$  at any nodes in the model was transiently simulated using a free Fortran program AC-UNSAF2D (Academic-UNsaturated-Saturated Analysis program by Finite element method-2Dimension), which was developed at Okayama University, Japan ([http://gw.civil.okayama-u.ac.jp/gel\\_home/](http://gw.civil.okayama-u.ac.jp/gel_home/)). AC-UNSAF2D is the most popular finite-element program for groundwater flow in Japan, because the program has been continuously improved from the 1970s. It is also compatible with available pre-post procedures, such as Geomodeler (GM Labo, Inc., Japan) which is used in this study. AC-UNSAF2D provides reasonable numerical simulation results owing to its optional algorithm for preserving the water balance equation, shown here as Eq. (8). Typically in the algorithm, the difference approximation for time discretization was made simply by the Euler method, and simulated  $H$  were assigned as variable boundary head conditions at each time step for the nodes along the screen interval. However, impermeable boundary conditions (black squares), representing the casing pipe, were set for the nodes above a depth of 5 m, at which mesh size associated with the well screen was changed from  $d_c/2$  to  $d_s/2$ . This study also implemented a model of the tube method, by extending the depth of the impermeable casing pipe to 6 m, and by assigning variable head boundary conditions for the nodes at the bottom only. This model represented the lower tube method and the simulated slug test data provided the conductivity estimate,  $\tilde{K}_{SL}$ . The upper tube method was not examined in this study, because the results in the upper tube method were approximately equivalent to those in the lower tube method in geometric terms, and can be obtained by changing  $K_T$  ( $K_6$ ),  $K_L$  ( $K_7$ ), and  $\tilde{K}_{SL}$ , to  $K_U$  ( $K_5$ ),  $K_T$  ( $K_6$ ), and  $\tilde{K}_{SU}$ , respectively.

The initial water level was assigned to be 1 m below the top of the model, and the initial drawdown  $H_0$  was generally 1 m, which was a drawdown from the initial 10 m domain head (10% of the aquifer thickness). It is considered that these test configurations are typical for shallow groundwater investigations. In contrast, the Hvorslev method was originally derived for an application in a confined formation. Thus, in the first analysis step described below,  $H_0$  was also set to 3 m for comparison to assess the error in an unconfined formation, as indicated in Brown et al. (1995). The boundary head was also kept constant at the initial head along the nodes opposite to the axis, as shown in Eq. (5). After the initial drawdown  $H_0$  in the well was given, the time interval for the simulation was 1 s for the period 1–10 s from the start, 10 s for the period 10–60 s, and 60 s from 60 to 1800 s. The error criterion on the hydraulic head for convergence was set to  $10^{-5}$  m in all nodes,

and the scale was equal to about one tenth of the minimum mesh size, as recommended in the program.

Two analysis steps were used to assess the effects of vertical flows from adjoining layers on conductivity estimates  $\tilde{K}_{HV}$  in the piezometer method, and  $\tilde{K}_{SL}$  in the lower tube method. The purpose in the first step was to validate the first assumption, and determine whether the conductivity estimates might be affected by the  $K_T$ ,  $K_U$ , and  $K_L$ , of the test, upper, and lower layers, respectively, but not by  $K_{U_i}$  and  $K_{L_i}$  ( $i = 2, 3, \dots$ ). In the first analysis, conductivity over the domain was assumed to be constant at  $10^{-5}$  m/s. Next, only one conductivity around the test layer, that is, one of  $K_4$ ,  $K_5$ ,  $K_6$ ,  $K_7$ , or  $K_8$ , was changed by one or two orders of magnitude (specifically, by  $10^{-7}$ ,  $10^{-6}$ ,  $10^{-4}$ , or  $10^{-3}$  m/s). Here,  $K_{U2}$ ,  $K_U$ ,  $K_T$ ,  $K_L$ , and  $K_{L2}$  in Fig. 1 correspond to  $K_4$ ,  $K_5$ ,  $K_6$ ,  $K_7$ , and  $K_8$  in this model, respectively. In each case, simulated slug test data were calculated by using the two-dimensional model in both the piezometer and lower tube methods. In the first step, the initial drawdown,  $H_0$ , in the well was set to either 1 or 3 m (corresponding to 4 and 2 m as the distance from the top of test screen) to show the effects of the unconfined conditions on Eqs. (11) and (12). Other flow parameter conditions were constant in the first step analysis: isotropy in each mesh, specific storage ( $10^{-5}$  in  $L^{-1}$ ), porosity (0.2 in dimensionless units). Parameters in the vadose zone above the water table, that is, unsaturated  $K$  and capillary pressure  $P$  versus volumetric water content  $\theta$ , were those reported by JICE (2012) for gravel deposits, as shown in Fig. 4. JICE (2012) summarized previous laboratory results of unsaturated  $K$  and  $P$  in various soils, and recommended the relations of unsaturated  $K$  and  $P$  with  $\theta$  in coarse and fine materials for engineering use. The relations were input into AC-UNSAF2D; however, we found that the simulations were not sensitive to these relations, owing to the high permeability of the saturated zone around the screen. Conductivity estimates for the piezometer and lower tube methods were calculated, and summarized as ratios to the actual conductivity  $K_T$ , that is,  $\tilde{K}_{HV}/K_T$  and  $\tilde{K}_{SL}/K_T$ .

The purpose of the second analysis step was to evaluate the second assumption, and to determine the constant parameters in Eqs. (13)–(15). In the piezometer method, conductivity  $K_T$  ( $K_6$  in Fig. 2) in the test layer was assigned to one of the three cases ( $10^{-4}$ ,  $10^{-5}$ , or  $10^{-6}$  m/s). Next, conductivity  $K_U$  and  $K_{U_i}$  ( $K_1$ – $K_5$ ) in all of the upper layers, or  $K_L$  and  $K_{L_i}$  ( $K_7$ – $K_{10}$ ) in all of the lower layers, were varied by

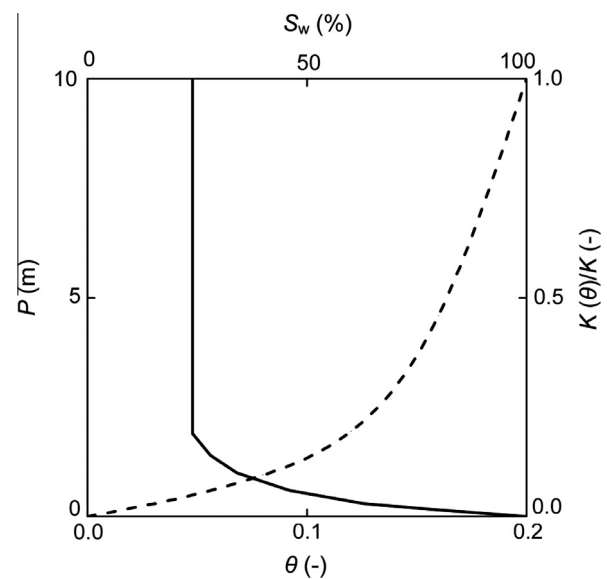


Fig. 4. Experimental curves of capillarity pressure head  $P$  (solid line) and unsaturated conductivity ratio  $K(\theta)/K$  (dashed line) versus volumetric water content  $\theta$  (degree of saturation  $S_w$ ) for unconsolidated gravel deposits.

two orders of magnitude in steps of half an order of magnitude. For example, when the conductivity of the test layer  $K_T$  was  $10^{-4}$  m/s, the conductivities of the upper or lower layers were chosen individually from  $10^{-2}$ ,  $10^{-2.5}$ ,  $10^{-3}$ ,  $10^{-3.5}$ ,  $10^{-4}$ ,  $10^{-4.5}$ ,  $10^{-5}$ ,  $10^{-5.5}$ , or  $10^{-6}$  m/s ( $9 \times 9 = 81$  patterns). As a result, 243 patterns were prepared in total for three values of  $K_T$ . The changes of conductivity in all of the upper or lower layers were approximately equal to those of only  $K_U$  or  $K_L$ , because of the insensitivity in the further upper and lower layers of  $K_{U_i}$  and  $K_{L_i}$ , as shown in the first step analysis. This simulation was also performed under anisotropic conditions (vertical  $K_z$  was one tenth of radial  $K_r$ ), and, thus, 486  $K$  patterns were used in total for the piezometer method. For simulating the lower tube method, the horizontal layers were divided into the lower and upper layers at the bottom of well. The conductivity in all of the lower layers,  $K_L$  and  $K_{L_i}$  ( $K_7$ – $K_{10}$ ) was set between  $10^{-2}$  and  $10^{-8}$  m/s, and those in all of the upper layers,  $K_T$ ,  $K_U$ , and  $K_{U_i}$  ( $K_1$ – $K_6$ ), were varied by two orders of magnitude from the conductivity in the lower layers. However, the maximum and minimum of conductivity for this analysis were  $10^{-2}$  and  $10^{-8}$  m/s, respectively, in the consideration of conductivity in alluvial gravel and sand (e.g., Freeze and Cherry, 1979). For example, when the conductivity in the lower layers was  $10^{-2}$  m/s, the conductivity in the upper layers was chosen from  $10^{-2}$ ,  $10^{-2.5}$ ,  $10^{-3}$ ,  $10^{-3.5}$ , and  $10^{-4}$  m/s (five patterns). As another example, when conductivity of the lower group was  $10^{-5}$  m/s, the conductivity of the lower group was chosen from  $10^{-3}$ ,  $10^{-3.5}$ ,  $10^{-4}$ ,  $10^{-4.5}$ ,  $10^{-5}$ ,  $10^{-5.5}$ ,  $10^{-6}$ ,  $10^{-6.5}$ , and  $10^{-7}$  m/s (nine patterns). Thus, the second step analysis for the tube method consisted of total 97 conductivity patterns in both isotropic and anisotropic conditions. After simulation, simulated head data in each  $K$  pattern were used to calculate the slopes,  $\log(H_1/H_2)/T$ , by a simple regression analysis. Next, the slopes were input into Eq. (11) or (12) to calculate conventional estimates  $\tilde{K}_{HV}$  and  $\tilde{K}_{SL}$ , and the estimates were divided by the conductivity  $K_T$  ( $K_6$ ) in the test layer. Finally, the constant parameters in Eqs. (13)–(15) were optimized individually in several groups of  $\tilde{K}_{HV}/K_T$  or  $\tilde{K}_{SL}/K_T$  by the least squares method. The groups were prepared for approximating the linear relationships with relatively high  $R^2$  values ( $R^2 \geq 0.7$ ) and low RMSE values (RMSE  $\leq 10\%$  of averaged  $\tilde{K}_{HV}/K_T$  or  $\tilde{K}_{SL}/K_T$ ). Finally, the results of this study were substantiated by recently reported field tests in the alluvial fan of the Toyohira River, Sapporo, Japan.

### 3. Results and discussion

#### 3.1. Sensitivity analysis results

Fig. 5 shows simulation results of the first step analysis in the piezometer (a) and tube (b) methods. Both hydraulic conductivity

ratios,  $\tilde{K}_{HV}/K_T$  and  $\tilde{K}_{SL}/K_T$ , were approximately independent of the initial drawdown,  $H_0$ , which was 1 or 3 m in this comparison. The insensitivity to initial drawdown means that the unconfined aquifer conditions might not be significant in this numerical simulation. Fig. 5a indicates that the Hvorslev estimate,  $\tilde{K}_{HV}$ , was  $1.06 \times 10^{-5}$  m/s under the assumption of a homogeneous formation, where all conductivity was  $10^{-5}$  m/s. The overestimate of the conductivity was similar to the results reported by Kono and Nishigaki (1983), and the value was probably caused by errors arising from the assumption of radial flow alone in Eq. (11). However, this error was within 10%, and thus was not significant in terms of the practical use of slug tests. Fig. 5a also indicates that  $\tilde{K}_{HV}/K_T$  depended on  $K_U$  and  $K_L$ , but not on  $K_{U2}$  and  $K_{L2}$ . This means that the estimate  $\tilde{K}_{HV}$  reflected conductivity only in the test layer, the upper adjoining layer, and lower adjoining layer; the first assumption was evaluated for the piezometer method. Furthermore,  $\tilde{K}_{HV}/K_T$  varied almost linearly with  $K_T$  in the test layer. However, the slope of  $\tilde{K}_{HV}/K_T$  was smaller for small  $K_T$  than for large  $K_T$ , because the groundwater discharge into the well  $Q_g$  remained owing to vertical flows from the adjoining layers. The simulated slug test data was dependent on relatively high conductivity in the adjoining upper and lower layers, even if  $K_T$  in the test layer was relatively small.  $\tilde{K}_{HV}/K_T$  also increased as  $K_U$  and  $K_L$  increased relative to  $K_T$ , but did not decrease as  $K_U$  and  $K_L$  decreased relative to  $K_T$ . It was expected that vertical flows would produce measurement error in the Hvorslev estimates only when the conductivity in the adjoining layer,  $K_U$  or  $K_L$ , was large relative to  $K_T$  in the test layer. In particular, the effect of vertical flows became significant when  $K_U$  or  $K_L$  was over one order of magnitude larger than  $K_T$ , and  $K_L$  had a greater effect than  $K_U$ , because vertical flows were more significant from the adjoining lower layer into the open bottom of the partially penetrating borehole.

Fig. 5b indicates that the Schmidt estimate  $\tilde{K}_{SL}$  was  $0.81 \times 10^{-5}$  m/s under the assumption of a homogeneous formation, that is, that  $K$  in all layers was constant at  $10^{-5}$  m/s. This value was about 20% smaller than the actual value ( $10^{-5}$  m/s), which was similar to the results of the previous study (Kono and Nishigaki, 1983). The underestimate was due to the impermeability of the casing pipe, which prevented the ideal concept of spherical flows assumed by Schmidt (1967). This error was several times larger than that of the Hvorslev method, and thus the piezometer method would be recommended when one is unsure which of the piezometer and tube methods to perform. Fig. 5b shows that  $\tilde{K}_{SL}$  depended on only  $K_T$  and  $K_L$ , and that there was no dependence of  $\tilde{K}_{SL}/K_T$  on the conductivities in other layers,  $K_U$ ,  $K_{U2}$ , and  $K_{L2}$ . These results are probably also appropriate for  $\tilde{K}_{SU}/K_U$  in the upper tube method;

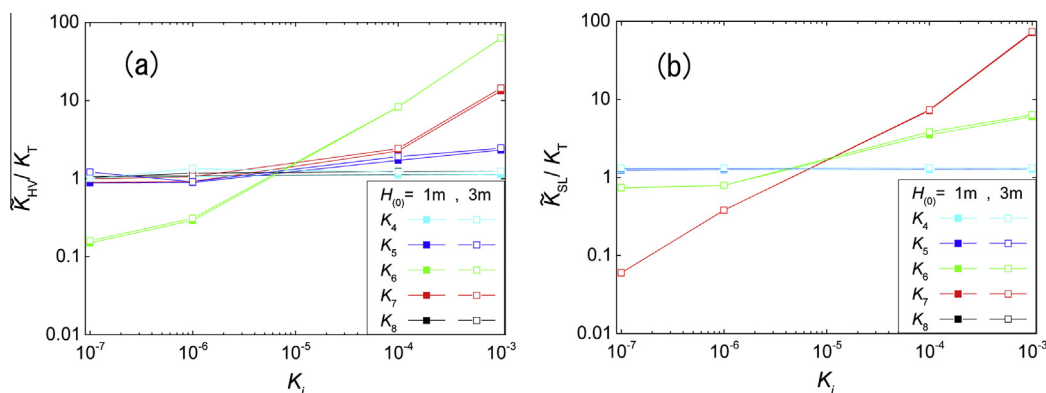


Fig. 5. Relations between conductivity in each layer and conductivity ratio (conductivity estimate over actual value) in the piezometer method (a) and the lower tube method (b). Units of conductivity and conductivity ratio are meters per second and dimensionless, respectively.

$\tilde{K}_{SU}$  would depend on the conductivity values of adjacent layers at the bottom, mainly on  $K_T$ , partly on  $K_U$ , but not on  $K_{U2}$ ,  $K_L$ , and  $K_{L2}$ . Thus, this study considered the validity of the first assumption with the tube method, as well as with the piezometer method. Fig. 5b also showed that  $\tilde{K}_{SL}/K_T$  increased almost linearly as  $K_L$  increased, due to the bottom being open to the lower adjoining layer. However, the slope was relatively small when  $K_L$  was smaller than  $K_T$ , owing to the vertical flows from the upper adjoining layer.

3.2. Parameter estimation results

Fig. 6 shows the simulation results of the second analysis step in the piezometer method, based on the isotropic condition ( $K_2/K_T = 1$ ). The colored surface was drawn using averages of  $\tilde{K}_{HV}/K_T$  for each value of  $K_U$  and  $K_L$  at  $10^{-4}$ ,  $10^{-5}$ , and  $10^{-6}$  m/s. The horizontal axes are given in terms of the logarithms of the conductivity ratios,  $R_U = \log(K_U/K_T)$  and  $R_L = \log(K_L/K_T)$ . Error bars on the surface indicate ranges of  $\tilde{K}_{HV}/K_T$  for three  $K_T$  patterns. The difference in three conductivity patterns was almost the same, at 0.2 or less in most patterns, except when  $K_L$  was two orders of magnitude larger than  $K_T$ . In such cases, the difference was from 0.3 to 0.5, but was still within 10% because  $\tilde{K}_{HV}/K_T$  also increased to more than 10. Therefore, we considered that the relation between  $\tilde{K}_{HV}/K_T$  and  $R_U$  or  $R_L$  was constant for  $K_T = 10^{-4}$ ,  $10^{-5}$ , and  $10^{-6}$  m/s. As indicated in Fig. 5a,  $\tilde{K}_{HV}/K_T$  increased with  $R_U$  and  $R_L$ , and the increments were more sensitive to  $R_L$  than to  $R_U$  because the base of the borehole was open to the lower adjoining layer. Fig. 5a shows that the surface was not a plane, indicating that the linear relation in Eq. (13) could not be confirmed over the entire domain of  $R_U$  and  $R_L$ . However, we could assume linear relations as approximately holding by classifying the results into three groups in terms of  $K_U/K_T$  and  $K_L/K_T$ : (1)  $K_L/K_T > 10$ ; (2)  $K_L/K_T \leq 10$  and  $K_U/K_T > 1$ ; and (3)  $K_L/K_T \leq 10$  and  $K_U/K_T \leq 1$ . Table 1 summarizes the constants determined by the least squares method for each group. Table 1 also shows RMSE and  $R^2$  as a result of the optimization. The  $R^2$  value was commonly over 0.7, and RMSE was within about 10% of  $\tilde{K}_{HV}/K_T$ . This study considered that these values indicated that Eq. (13) was a reasonable approximation in each group of  $K_U/K_T$  and  $K_L/K_T$ .

Fig. 7a and b illustrates simulation results from the second step for the upper (a) and lower (b) tube methods, respectively. These

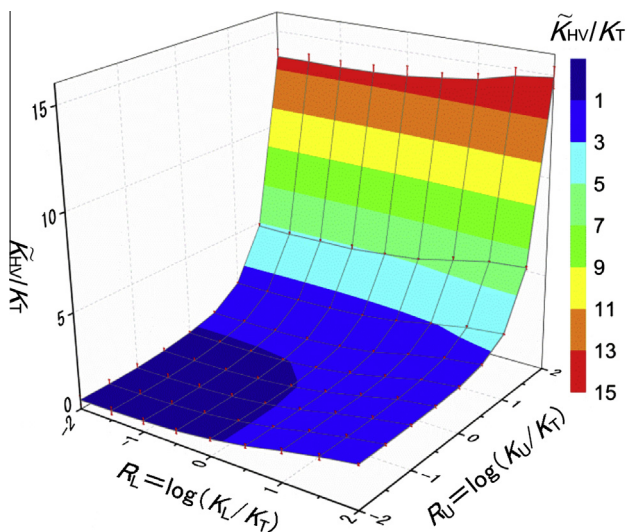


Fig. 6. Sensitivity analysis results in the piezometer method for various patterns of  $K_U$  and  $K_L$ .

Table 1

Numerical simulation results as optimum parameters in Eqs. (13)–(15) under an isotropic condition.

Conductivity ratio	Conditions		Parameters			$R^2$	RMSE
	$K_U/K_T$	$K_L/K_T$	$a$	$b$	$c$		
$\tilde{K}_{HV}/K_T$	>10	>10	0.35	11.55	-10.00	0.91	1.50
	>1	$\leq 10$	0.69	0.18	1.11	0.93	0.11
	$\leq 1$	$\leq 10$	0.15	0.25	1.14	0.74	0.13
$\tilde{K}_{SU}/K_T$	>1		1.65		0.68	0.98	0.27
	$\leq 1$		0.16		0.70	0.73	0.08
$\tilde{K}_{SL}/K_T$	>10	>10	61.29	-77.40	1.00	0.97	
	>1	>1	4.01	0.44	0.91	0.53	
	$\leq 1$	$\leq 1$	0.38	0.69	0.91	0.09	

results were obtained for the isotropic condition. In both methods, the estimates in the tube methods were related mainly to conductivity in the lower adjacent layer, that is  $K_T$  for  $\tilde{K}_{SU}$  and  $K_L$  for  $\tilde{K}_{SL}$ . As in the piezometer method, the linear relations in Eqs. (14) and (15) could not be obtained over the entire domain of  $R_U$  or  $R_L$ . However, the solid lines in Fig. 7 indicate that linear relations could be obtained when the simulation results were classified into several groups. In the upper tube method (Fig. 7a), two classes should be defined for the approximate linear relation in Eq. (14): (1)  $K_U/K_T > 1$ ; and (2)  $K_U/K_T \leq 1$ . In the lower tube method (Fig. 7b), three classes should be used for the relation in Eq. (15): (1)  $K_L/K_T > 10$ ; (2)  $K_L/K_T \leq 10$  and  $K_U/K_T > 1$ ; and (3)  $K_U/K_T \leq 10$  and  $K_U/K_T \leq 1$ . Table 1 also summarizes optimized constants obtained from the upper and lower tube methods.  $R^2$  values were sufficiently high (over 0.7), and RMSE values except for  $K_L/K_T > 10$  were small enough that relative errors were within 10% of  $\tilde{K}_{SU}/K_T$  and  $\tilde{K}_{SL}/K_T$ .

Table 2 shows the second step analysis results for the anisotropic condition ( $K_2/K_T = 0.1$ ), to reveal the sensitivity of this method to small-scale anisotropy within each layer. The anisotropy ratio was given as the upper bound of that on a small scale; the anisotropy ratio of a hydrologic unit within 1 m of thickness is often reported as between 0.1 and 1 (e.g., Freeze and Cherry, 1979; Burger and Belitz, 1997). It should be noted that the conductivity estimates in Eqs. (11) and (12) were calculated based on the isotropic condition ( $K_2/K_T = 1$ ). All constants except  $b$  and  $c$  were similar to or slightly smaller than those for the isotropic condition (Table 1). In contrast, the constants  $b$  and  $c$  were almost half of those in the case of  $K_L/K_T > 10$ , which is due to the suppression of vertical flow into the bottom. Although the Hvorslev method has been considered to be insensitive to anisotropy (Butler, 1997), the difference in these stratified aquifers indicates that the methodology has the potential to provide information, not only about large-scale heterogeneity such as stratified formations, but about small-scale anisotropy within the length of a well screen; the development of this potential remains for future study.

3.3. Recommendations

When slug tests are performed in the test interval layer with the piezometer method and at the upper and lower boundary depths with the tube method, actual conductivity  $K_T$  can be estimated based on three measurements using Eqs. (13)–(15) with the constants in Tables 1 or 2. This study also suggests combining the piezometer and tube methods by installing casing pipe in 1 m sections during the drilling procedure. First, the casing is lowered to the bottom of the borehole, and  $\tilde{K}_{SU}$  is obtained with the tube method. Next, the open interval is constructed by core sampling for 1 m, and  $\tilde{K}_{HV}$  is obtained using the piezometer method. The

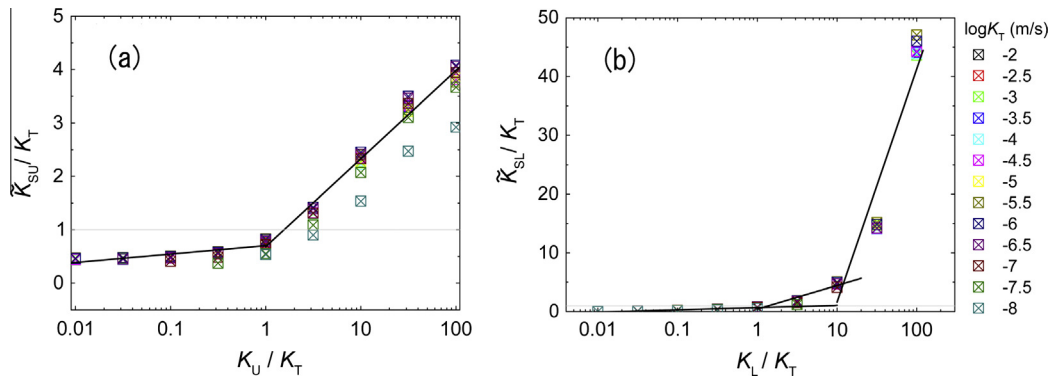


Fig. 7. Sensitivity analysis results in the upper tube method (a) and the lower tube method (b).

Table 2  
Optimum parameters in an anisotropic condition ( $K_z/K_T = 0.1$ ).

Conductivity ratio	Conditions		Parameters			$R^2$	RMSE
	$K_U/K_T$	$K_L/K_T$	$a$	$b$	$c$		
$\tilde{K}_{HV}/K_T$	>10		0.30	5.77	-4.57	0.92	0.73
	>1	$\leq 10$	0.61	0.10	0.69	0.96	0.07
	$\leq 1$	$\leq 10$	0.07	0.13	0.81	0.67	0.08
$\tilde{K}_{SU}/K_T$	>1		1.67		0.21	0.97	0.28
	$\leq 1$		0.10		0.40	0.69	0.05
$\tilde{K}_{SL}/K_T$	>10		32.71		-41.36	1.00	0.41
	>1		2.07		0.28	0.90	0.29
	$\leq 1$		0.21		0.41	0.94	0.05

casing pipe is lowered to the bottom of the borehole again, and  $\tilde{K}_{SL}$  is obtained at that depth. As  $\tilde{K}_{SL}$  also contributes to  $\tilde{K}_{SU}$  for the lower layer, the next step is to use the piezometer method over a meter long core in the lower layer. The cycle continues, and thus a series of  $\tilde{K}_{HV}$  and  $\tilde{K}_{SL}$  ( $=\tilde{K}_{SU}$ ) values is obtained. This series of partially penetrating slug test results is then translated using Eqs. (13)–(19), so that the vertical variation in  $K$  is represented more reasonably than by measurements alone.

3.4. Uncertainty and limitations

We emphasized the efficiency of this proposed method above, but several problems and uncertainties should be discussed. First, the linear relations, Eqs. (13)–(15), are fundamental to this method. However, they were not validated theoretically, so the constants were numerically determined only for specific types of borehole conditions and conventional solutions. It is necessary for the linear relations to be derived analytically from basic flow equations and boundary conditions, and for the constants to be calculated for any patterns of heterogeneity, borehole configurations, and conventional solutions (e.g., Cooper et al., 1967, Bouwer and Rice, 1976). Second, Table 1 or 2 required information about  $K_U/K_T$  and  $K_L/K_T$ , but such information cannot be obtained in advance. A practical approach is to use a series of measurements of  $\tilde{K}_{HV}$  instead of  $K_T$ ,  $K_U$ , and  $K_L$ , for estimating  $K_U/K_T$  and  $K_L/K_T$ . Once  $K_T$  values are estimated from the tentative  $K_U/K_T$  and  $K_L/K_T$  values,  $K_U/K_T$  and  $K_L/K_T$  could be replaced, and the constants in Table 1 or 2 determined again. It might seem effective to apply an iterative process for obtaining convergence of  $K$  within a given criterion. However, such an iterative process will not necessarily converge, because Eqs. (13)–(15) include errors as shown in Tables 1 and 2. In particular, around the condition of  $K_L/K_T = 1$ , the solutions might change suddenly, and lead to an instability in

the iteration. The approximately linear models in Eqs. (13)–(15) were useful for obtaining straightforward solutions, but were not rigorous because the simulated surface shown in Fig. 6 was smoothed. For more accuracy, the parameters in Tables 1 and 2 should be obtained from the smooth surface individually for each value of  $R_U$  and  $R_L$ . Considering this uncertainty, the vertical variations of  $K$  remain to be confirmed, by comparison with other field approaches, such as flow meters and pumping tests at different depths. Furthermore, this study assumed perfectly horizontal structures; however, we should consider the more realistic situation of discontinuous layers in both the horizontal and vertical directions, for example, fractured rocks. Future studies are required to evaluate and develop the methodology in three dimensions. Despite the uncertainty, it should be emphasized that incorporating the piezometer and tube methods has an advantage in terms of cost and convenience. The proposed method corrects for the effects of adjoining layers in heterogeneous formations, although not completely and with some uncertainty, and allows us to establish vertical variations of  $K$  more accurately than from single measurements.

3.5. Case study

Finally, a field example is introduced to indicate the effectiveness for the application of this method, especially in monotonic heterogeneous aquifers such as alluvial gravel deposits. Results from alternating multi-level slug tests were obtained for April 2013 in the alluvial fan of the Toyohira River, Sapporo, Japan. Fig. 8 shows topographic features around the Toyohira River alluvial fan. The alluvial fan is located at about 43°N, 141°E in Hokkaido, the northernmost island of Japan. The Toyohira River flows through Sapporo City, which has a population of 1.9 million, and forms an alluvial fan, with a longitudinal extent of about 7 km and an area of over 35 km<sup>2</sup>. There are unconfined gravel sequences, which constitute a groundwater reservoir with a total pumping rate of over 80,000 m<sup>3</sup>/d. River seepage is the main source for recharging groundwater (Hu et al., 2010; Sakata and Ikeda, 2012), and the filtration process from the river to the deeper levels is controlled by the depth-decaying permeability of gravel deposits on a scale of tens of meters (Sakata and Ikeda, 2013). However, Monte Carlo simulation revealed the importance of heterogeneity on a smaller scale (1 m) for interpreting heat transport between surface water and groundwater (Sakata, 2015). A series of partially penetrating slug tests were performed to assess the small-scale heterogeneity of the gravel deposits.

Piezometer and tube measurements were performed in the drilling procedure at depths between five and 11 m at intervals of 1 m at the fan apex (Fig. 8). The water table appeared at a depth of 4.5 m, and was almost stable at that depth during the series of slug

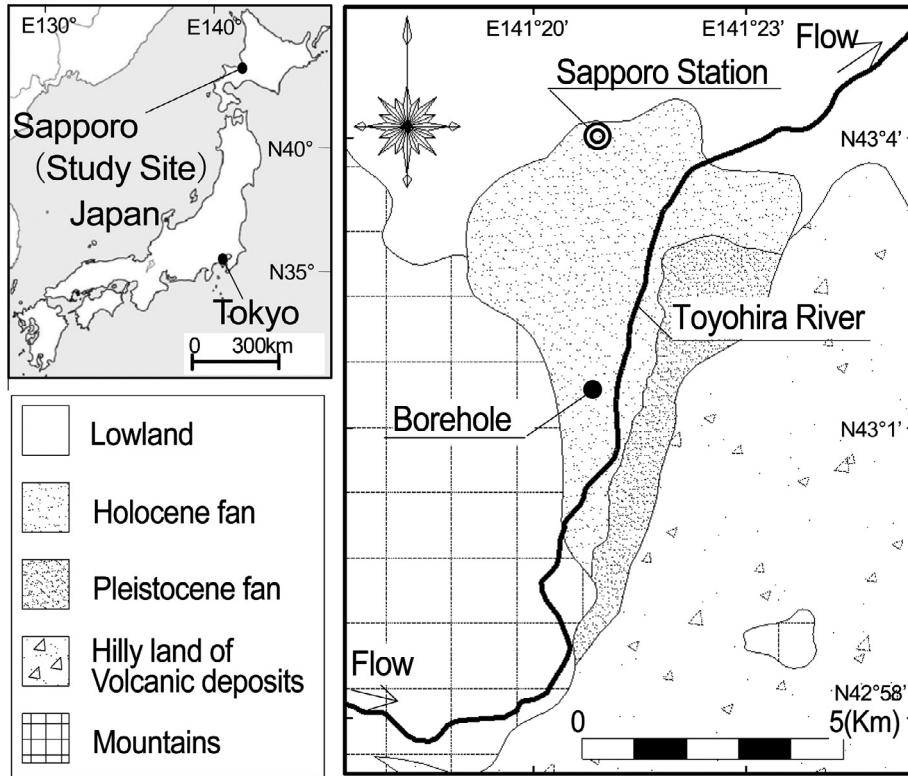


Fig. 8. Topographic map of the Toyohira River alluvial fan, indicating the borehole location for a series of slug tests.

**Table 3**  
A field example of a series of slug test results obtained by the piezometer and tube methods, in the alluvial fan of the Toyohira River, Japan.

Layer (ith)	Depth (m)	$\bar{K}_{HV}$ (m/s)	$\bar{K}_{SU}$ (m/s)	$\alpha_U$ (-)	$\alpha_L$ (-)	$R_U$ (-)	$R_L$ (-)	$\bar{K}_T$ (m/s)	$\bar{R}_L$ (-)	$ \bar{R}_L - R_L $ (-)
1	4.6–5	$5.42 \times 10^{-3}$								
2	5–6	$1.16 \times 10^{-3}$	$1.93 \times 10^{-4}$	6.01	266.84	-0.36	-1.83	$2.19 \times 10^{-3}$	-1.21	0.62
3	6–7	$8.66 \times 10^{-5}$	$4.35 \times 10^{-6}$	19.92	2.27	-0.39	-1.09	$1.35 \times 10^{-4}$	-1.57	0.48
4	7–8	$3.36 \times 10^{-5}$	$3.82 \times 10^{-5}$	0.88	0.68	5.96	1.49	$3.63 \times 10^{-6}$	2.76	1.27
5	8–9	$1.03 \times 10^{-3}$	$4.95 \times 10^{-5}$	20.87	0.87	-4.30	0.03	$2.08 \times 10^{-3}$	0.50	0.47
6	9–10	$1.23 \times 10^{-3}$	$1.18 \times 10^{-3}$	1.04	11.80	-3.32	-1.80	$6.59 \times 10^{-3}$	-1.78	0.02
7	10–11	$1.10 \times 10^{-4}$	$1.04 \times 10^{-4}$							

tests. Table 3 shows conductivity estimates from the piezometer and tube methods, and modified  $\bar{K}_T$  values from Eqs. (13)–(19). In Table 3,  $\bar{R}_L$  is the logarithmic ratio of the modified estimates of  $\bar{K}_T$  in the layer and lower adjoining layer:  $\bar{R}_L$  in the layer 5–6 m in depth was  $\log(1.35 \times 10^{-4}/2.19 \times 10^{-3}) = -1.21$ .  $|\bar{R}_L - R_L|$  denotes the magnitude of the difference between  $R_L$  and  $\bar{R}_L$ , and this value indicates the estimation error in this solution. Fig. 9 shows results from the piezometer method  $\bar{K}_{HV}$  (black lines) and from the tube method  $\bar{K}_{SU}$  (black solid blocks). The red lines in Fig. 9 indicate modified conductivity estimates,  $\bar{K}_T$ , with error bars of  $|\bar{R}_L - R_L|$ . Conductivity estimates,  $\bar{K}_{HV}$ , in the piezometer (Hvorslev) method varied several times by over one order of magnitude, even at adjacent depth intervals. These large variations indicate geological heterogeneity in the alluvial fan gravel deposits. In the vertical variation, highly permeable layers were identified at 4.6–6 m and 8–10 m. In particular, the upper layer was considered to be the beginning of an exponentially decaying trend in the gravel sequences. However, less permeable layers were found at depths of 7–8 m and 10–11 m. Conductivity estimates in the layers were in the order of  $10^{-5}$  m/s, and the values were not small

enough for layers to be impermeable. However, the conductivity was about two orders of magnitude smaller than that in other layers. Thus, the layers might serve as aquitards in the shallow unconfined aquifer, and prevent vertical flows infiltrating the deeper parts.

Modified conductivities,  $\bar{K}_T$ , estimated by this method approximately corresponded with the measurements of  $\bar{K}_{HV}$  at depths of 5–6 m, 6–7 m, and 8–9 m; the discrepancy between measured and estimated conductivity was no more than twofold. In contrast, there was a significant discrepancy in two layers. In the upper layer at 7–8 m, the modified conductivity ( $\bar{K}_T = 3.6 \times 10^{-6}$  m/s) was almost one order of magnitude smaller than the measured conductivity ( $\bar{K}_{HV} = 3.4 \times 10^{-5}$  m/s). The overestimate in the measurement was due to the effect of a lower adjoining layer of relatively high permeability (8–9 m in depth). Also, in the lower layer at 9–10 m, the estimated value ( $\bar{K}_T = 6.6 \times 10^{-3}$  m/s) was about 5 times larger than the measured value ( $\bar{K}_{HV} = 1.2 \times 10^{-3}$  m/s). The underestimate was also due to a lower adjoining layer of low permeability (10–11 m in depth). These differences indicate that the actual  $K$  variation might be affected not only by permeability in each test layer, but also by permeability in the adjoining upper and lower

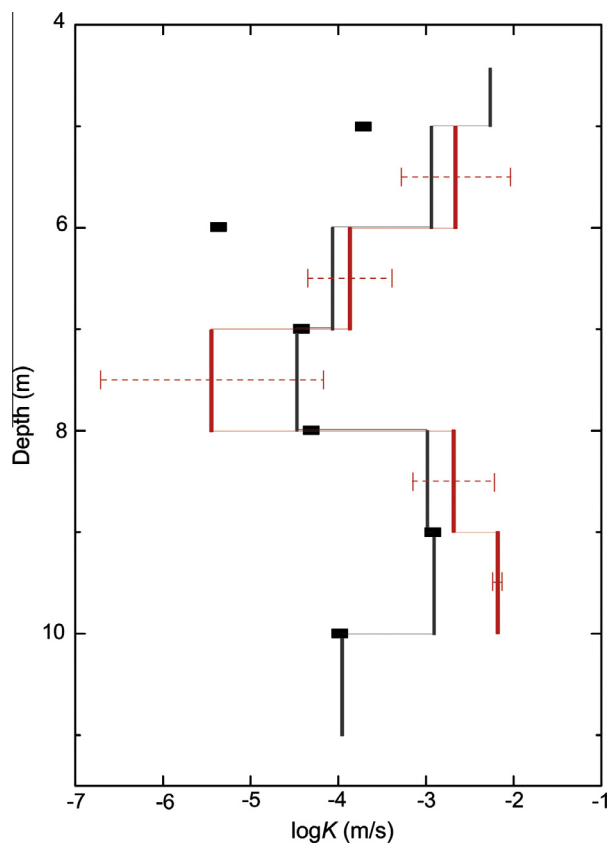


**Fig. 9.** Comparison between measured and modified values of hydraulic conductivity in a borehole in the Toyohira River alluvial fan. Black lines denote the conductivity estimate from the piezometer method, and black solid blocks denote estimates from the tube method. Red lines denote modified conductivity with error bars, calculated from  $|R'_i - R_i|$  in Table 3. Units of depth and  $\log K$  are meters and meters per second, respectively.

layers. In other words, the measured  $\tilde{K}_{HV}$  variations were probably smoothed as a result of the effects of adjoining layers of different permeability and the vertical variations of  $K$  would fluctuate more widely than was indicated by the measurements. Although the results contain uncertainties, this interpretation would be key information for evaluating extremely permeable layers, including preferential flow paths, and low permeability aquitards controlling water infiltration to deeper parts.

#### 4. Conclusions

In this study we performed a numerical sensitivity analysis of partially penetrating slug tests for various patterns of permeability in a horizontally layered system. This study considered borehole configurations for two types of methods: the piezometer and tube methods. The thickness of each layer was assumed to be 1 m, which was equal to the test screen length in the piezometer method. Conductivity estimates were calculated from numerically simulated slug test data by conventional solutions obtained under the homogeneity assumption. Conductivity estimates were compared to actual values, assuming linear relations to create an efficient method by alternating the piezometer and tube methods. As a result, the following conclusions were obtained.

- (1) Conductivity estimates in the piezometer method,  $\tilde{K}_{HV}$ , were dependent mainly on  $K_T$  in the test layer corresponding to the test screen. The estimate was also affected by the conductivities in the upper and lower adjacent layers,  $K_U$  and

$K_L$ , especially when these values were relatively large. Conductivity estimates in the tube method,  $\tilde{K}_{SL}$ , were linearly affected by conductivity in the lower layer open to the bottom,  $K_L$ , but were also influenced by the upper adjoining layer,  $K_T$ , when the value was relatively large. The effects of conductivity in further lower and upper layers were almost negligible in both the piezometer and tube methods.

- (2) Conductivity ratios (conductivity estimate to actual value) were approximated by linear relations of logarithms of actual conductivity values in the test layer, upper and lower adjoining layers,  $K_T$ ,  $K_U$ , and  $K_L$ . Although the relations were originally inferred from the previous study in the analytical solutions based on vertical uniformity, this numerical sensitivity analysis shows the validity with sufficient accuracy in practice. A conductivity estimate could be readily found by obtaining three measurements: one with the piezometer method, and two with the tube method at the top and bottom of the test screen. For the anisotropic condition, the parameters in the linear relations were almost half those under isotropic conditions, indicating the potential to examine such small-scale anisotropic conditions even during the partially penetrating slug tests.
- (3) We proposed performing a series of partially penetrating slug tests, alternating the piezometer and tube methods, so that vertical variations of  $K$  would be obtained more accurately than by single measurements. In a case study of the Toyohira River alluvial fan, Japan, the approach could reveal an extremely highly permeable layer as preferential flow paths and low permeability layers as aquitards, contributing to the interpretation of vertical heterogeneity in the gravel deposits. As in this case study, this method will be effective in a typical case in which a series of slug tests in a borehole procedure shows a large variability of  $K$  (e.g., several orders of magnitude) in monotonic sequences, so that it is often difficult to decide which depths slug tests should be performed at. This situation matches coarse alluviums and fractured rock, and that the hypothesis of stratified formations might be more appropriate for the former.

#### Acknowledgements

The authors thank our colleagues Prof. Kazuhisa K. Chikita and Prof. Shoshiro Minobe, who provided helpful comments which led to substantial improvements. We also sincerely thank the three anonymous reviewers for their insightful comments on this paper. Technical support for this analysis was received with gratitude from our graduate students, Takuto Miyamoto, Yasuhiro Ochiai, Hiroyuki Uehara, and Sho Makino, and our colleagues Kizaki Kenji, Hideki Otake, and Asaki Yoshida. ACE Shisui Co., Ltd., Japan, collected measurements in the case study. This work was financially supported by JSPS KAKENHI Grant Number 25920014.

#### References

- Beckie, R., Harvey, C.F., 2002. What does a slug test measure: an investigation of instrument response and the effects of heterogeneity. *Water Resour. Res.* 38 (12), 26-1–26-14. <http://dx.doi.org/10.1029/2001WR001072>.
- Black, J.H., 2010. The practical reasons why slug tests (including falling and rising head tests) often yield the wrong value of hydraulic conductivity. *Q. J. Eng. Geol. Hydrogeol.* 43, 345–358. <http://dx.doi.org/10.1144/1470-9236/08-094>.
- Bouwer, H., Rice, R.C., 1976. A slug test for determining hydraulic conductivity of unconfined aquifers with completely or partially penetrating wells. *Water Resour. Res.* 12 (3), 423–428. <http://dx.doi.org/10.1029/WR012i003p00423>.
- Brown, D.L., Narasimhan, T.N., Demir, Z., 1995. An evaluation of the Bouwer and rice method of slug test analysis. *Water Resour. Res.* 31 (5), 1239–1246. <http://dx.doi.org/10.1029/94WR03292>.

- Burger, R.L., Belitz, K., 1997. Measurement of anisotropic hydraulic conductivity in unconsolidated sands: a case study from a shoreface deposit, Oyster, Virginia. *Water Resour. Res.* 33 (6), 1515–1522. <http://dx.doi.org/10.1029/97WR00570>.
- Butler Jr., J.J., 1997. *The Design, Performance, and Analysis of Slug Tests*. Lewis Publishers, Boca Raton, Florida, 252p.
- Butler Jr., J.J., Bohling, G.C., Hyder, Z., McElwee, C.D., 1994. The use of slug tests to describe vertical variations in hydraulic conductivity. *J. Hydrol.* 156 (1–4), 137–162. [http://dx.doi.org/10.1016/0022-1694\(94\)90075-2](http://dx.doi.org/10.1016/0022-1694(94)90075-2).
- Butler Jr., J.J., Zhan, X., 2004. Hydraulic tests in highly permeable aquifers, *Water Resour. Res.* 40. <http://dx.doi.org/10.129/2003WR002998>, W12402.
- Cardiff, M., Barrash, W., Thoma, M., Malama, B., 2011. Information content of slug tests for estimating hydraulic properties in realistic, high-conductivity aquifer scenarios. *J. Hydrol.* 403 (1–2), 66–82. <http://dx.doi.org/10.1016/j.jhydrol.2011.03.044>.
- Chen, C.S., Wu, C.R., 2006. Analysis of depth-dependent pressure head of slug tests in highly permeable aquifers. *Groundwater* 44 (3), 472–477. <http://dx.doi.org/10.1111/j.1745-6584.2005.00152.x>.
- Cheng, A.H.D., Morohunfolo, O., 1993. Multilayered leaky aquifer systems 1. Pumping well solutions. *Water Resour. Res.* 29 (8), 2787–2800. <http://dx.doi.org/10.1029/93WR00768>.
- Cooper Jr., H.H., Bredehoeft, J.D., Papadopoulos, I.S., 1967. Response of a finite-diameter well to an instantaneous charge of water. *Water Resour. Res.* 3 (1), 263–269. <http://dx.doi.org/10.1029/WR003i001p00263>.
- Fetter, C.W., 2001. *Applied Hydrogeology*, fourth ed. Prentice-Hall, Upper Saddle River, pp. 193–197.
- Freeze, R.A., Cherry, J.A., 1979. *Groundwater*. Prentice-Hall, Englewood Cliffs, New Jersey.
- Gelhar, L.W., 1993. *Stochastic Subsurface Hydrology*. Prentice-Hall, Englewood Cliffs, New Jersey, pp. 290–297.
- Hemker, C.J., 1999. Transient well flow in vertically heterogeneous aquifers. *J. Hydrol.* 225, 1–18. [http://dx.doi.org/10.1016/S0022-1694\(99\)00137-7](http://dx.doi.org/10.1016/S0022-1694(99)00137-7).
- Hu, S.G., Miyajima, S., Nagaoka, D., Koizumi, K., Mukai, K., 2010. Study on the relation between groundwater and surface water in Toyohira-gawa alluvial fan, Hokkaido, Japan. In: Taniguchi, M., Holman, I.P. (Eds.), *Groundwater Response to Changing Climate*. CRC Press, London, pp. 141–158.
- Hvorslev, M.J., 1951. Time lag and soil permeability in ground water observations. U.S. Army Engineering Water ways Experimental Station, Bulletin 36, Vicksburg, Mississippi, 50 p.
- Hyder, Z., Butler Jr., J.J., McElwee, C.D., Liu, W., 1994. Slug tests in partially penetrating wells. *Water Resour. Res.* 30 (11), 2945–2957. <http://dx.doi.org/10.1029/94WR01670>.
- JICE (Japan Institute of Construction Engineering), 2012. *Manual for the design of river structures in Japan*. JICE Reports, 51–57, No. 111002.
- Karasaki, K., Long, C.S., Witherspoon, P.A., 1988. Analytical models of slug tests. *Water Resour. Res.* 24 (1), 115–126. <http://dx.doi.org/10.1029/WR024i001p00115>.
- Koltermann, C.E., Gorelick, S.M., 1995. Fractional packing model for hydraulic conductivity derived from sediment mixtures. *Water Resour. Res.* 31 (12), 3283–3297. <http://dx.doi.org/10.1029/95WR02020>.
- Kono, I., Nishigaki, M., 1983. Some studies on the analyses of in-situ permeability tests. *Soils Found.* 23 (4), 157–170.
- Leek, R., Wu, J.Q., Wang, L., Hanrahan, T.P., Barber, M.E., Qiu, H., 2009. Heterogeneous characteristics of streambed saturated hydraulic conductivity of the Touchet River, south eastern Washington, USA. *Hydrol. Process.* 23 (8), 1236–1246. <http://dx.doi.org/10.1002/hyp.7258>.
- Maas, C., 1987. Groundwater flow to a well in a layered porous medium: 1. Steady flow. *Water Resour. Res.* 23 (8), 1675–1681. <http://dx.doi.org/10.1029/WR023i008p01675>.
- Malama, B., Barrash, W., Cardiff, M., Thoma, M., Kuhlman, K.L., 2011. Modeling slug tests in unconfined aquifers taking into account water table kinematics, wellbore skin and inertial effects. *J. Hydrol.* 408 (1–2), 113–126. <http://dx.doi.org/10.1016/j.jhydrol.2011.07.028>.
- Ross, H.C., McElwee, C.D., 2007. Multi-level slug tests to measure 3-D hydraulic conductivity distributions. *Nat. Resour. Res.* 16 (1), 67–79. <http://dx.doi.org/10.1007/s11053-007-9034-9>.
- Rovey, C.W., Cherkauer, D.S., 1995. Scale dependency of hydraulic conductivity measurements. *Groundwater* 33 (5), 769–780. <http://dx.doi.org/10.1111/j.1745-6584.1995.tb00023.x>.
- Sakata, Y., 2015. Heat as a tracer for examining depth-decaying permeability in gravel deposits. *Groundwater* 53, 21–31. <http://dx.doi.org/10.1111/gwat.12236>.
- Sakata, Y., Ikeda, R., 2012. Quantification of longitudinal river discharge and leakage in an alluvial Fan by synoptic survey using handheld ADV. *J. Jpn. Soc. Hydrol. Water Resour.* 25, 89–102.
- Sakata, Y., Ikeda, R., 2013. Depth dependence and exponential models of permeability in alluvial fan gravel deposits. *Hydrogeol. J.* 21 (4), 773–786. <http://dx.doi.org/10.1007/s10040-013-0961-8>.
- Schmidt, W.E., 1967. Field determination of permeability by the infiltration test. In: Johnson, A.I. (Ed.), *Permeability and Capillarity of Soils*. American Society of Testing and Materials, Baltimore, pp. 142–157.
- Shapiro, A.M., Hsieh, P.A., 1998. How good are estimates of transmissivity from slug tests in fractured rock? *Groundwater* 36 (1), 37–48. <http://dx.doi.org/10.1111/j.1745-6584.1998.tb01063.x>.
- Yu, Y.H., Lloyd, J.W., 1992. A multi-layered radial flow model interpretation of drill stem test data. *J. Hydrol.* 136, 73–86. [http://dx.doi.org/10.1016/0022-1694\(92\)90005-G](http://dx.doi.org/10.1016/0022-1694(92)90005-G).
- Zemansky, G.M., McElwee, C.D., 2005. High-resolution slug testing. *Groundwater* 43 (2), 222–230. <http://dx.doi.org/10.1111/j.1745-6584.2005.00008.x>.
- Zlotnik, V.A., Zurbuchen, B.R., 2003. Field study of hydraulic conductivity in a heterogeneous aquifer: comparison of single-borehole measurements using different instruments. *Water Resour. Res.* 39 (4), 1101. <http://dx.doi.org/10.1029/2002WR001415>.